Electrical Anisotropy Below Slow- and Fast-Moving Plates: Paleoflow in the Upper Mantle?

Karsten Bahr[1]* and Fiona Simpson[2]

Upper mantle electrical conductivities can be explained by hydrogen diffusivity in hydrous olivine. Diffusivity enhances the conductivity of olivine anisotropically, making the *a* axis the most conductive of the three axes. Therefore, the hypothesis that plate motion induces lattice-preferred orientation of olivine can be tested with the use of long-period electromagnetic array measurements. Here, we compared electrical anisotropies below the slow-moving Fennoscandian and fast-moving Australian plates. The degree of olivine alignment is greater in the mantle below the Fennoscandian plate than below the Australian plate. This finding may indicate that convection rather than plate motion is the dominant deformation mechanism.

Paleomagnetic data can constrain the position and orientation of plates over geological time scales, whereas azimuthal variations of Rayleigh wave phase velocities have been inferred to indicate present-day mantle flow at the base of the lithosphere (*1*). Here we show that an electrically anisotropic mantle could provide a link between past plate trajectories and present-day mantle flow directions. Long-period magnetotelluric field studies indicate the presence of electrical anisotropy in the upper mantle beneath the Canadian Shield (*2*), Central Europe (*3*), and Australia (*4*), which may be generated by grain-scale anisotropy of hydrous olivine crystals (*5, 6*) or by conducting graphite films oriented along grain boundaries within macroscopic shear zones (*2*).

Coincidence between the electromagnetic strike (the direction of highest conductance) at long (10,000 s) periods (*4*) and the fast direction obtained from anisotropy studies of seismic shear waves at 150 to 200 km depth under central Australia (*7*) indicates strain-induced alignment of olivine crystals. However, there is a 27° discrepancy between the electromagnetic strike [estimated with 7° confidence intervals (*4*)] and the present-day plate motion direction of Australia. This discrepancy contradicts the assumption that this alignment is an immediate response to the relatively fast present-day motion of the Australian plate, and it could indicate a resistance to deformation of the mantle by plate motion (*4*) or more complicated effects arising from mantle convection.

We present evidence for electrical anisotropy in the sublithospheric mantle below Fennoscandia based on long-period electromagnetic array data from 22 sites (Fig. 1). The electromagnetic strike at each site is estimated by finding the direction that maximizes the splitting of the impedance phases (*3, 4*). Array data are needed to distinguish between a model incorporating azimuthal electrical anisotropy under the lithosphere and an alternative model involving a laterally displaced conductivity anomaly. In both cases, the impedance phases will be split in two principal polarization directions, with the larger impedance phase attributed to the higher conductance direction. But in the deep anisotropic case, the degree of impedance phase splitting will remain the same over large distances, whereas in the case of a laterally displaced conductivity anomaly the impedance phase splitting will decrease with distance from the anomaly. Changes in the amount of phase splitting from site to site (Fig. 1) indicate some lateral variation of the conductance in the high-conductivity direction, but the direction itself is stable over large distances. The high-conductance directions group around 35° away from north to the east under Sweden and 45° away from north to the east under Finland. The application of the error propagation to the strike direction estimation (*8*) yields angular errors less than 10°. The result for Sweden is in reasonable agreement with azimuthal anisotropy obtained from shear wave splitting (*9*).

Laterally displaced conductivity anomalies generate geomagnetic transfer functions that correlate with the occurrence of the impedance phase split (*10*). Horizontal geomagnetic transfer functions (Fig. 2) are dimensionless measures of the amplitude of time-varying geomagnetic fields (*11*) recorded si-

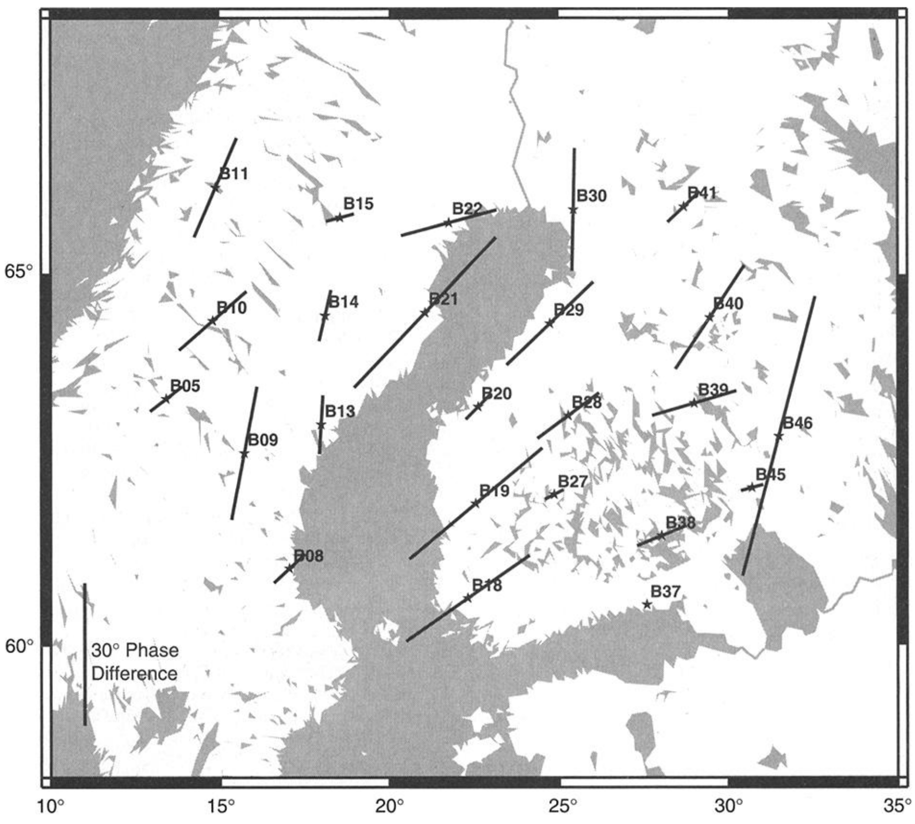

Fig. 1. Map showing locations of magnetotelluric stations (stars). The line through each station shows the electromagnetic strike at period 2049 s, corresponding to 180 km depth. The length of the bars indicates the amount of phase splitting, $\phi_{xy} - \phi_{yx}$ (*2*).

[1]Geophysics Institute, University of Göttingen, 37075 Göttingen, Germany. [2]Institute of Geological and Nuclear Sciences, 69 Gracefield Road, Lower Hutt, New Zealand.

*To whom correspondence should be addressed. E-mail: kbahr@uni-geophys.gwdg.de

multaneously at all sites in the array. Impedance phase splitting, which occurs at all sites in the array (Fig. 1), is not correlated with the geomagnetic transfer functions. Therefore, deep anisotropy is necessary to explain the impedance phase data.

Short-period electromagnetic fields penetrate less deeply into Earth than do fields with longer periods. Therefore, the period dependence of the electromagnetic strike can be used to distinguish between lithosphere and sublithospheric alignments (*3, 4*). This can help in resolving the ambiguity associated with the depth of anisotropy obtained from shear wave splitting analyses. However, magnetotelluric depth estimations are often hindered by local distortions of the electric field amplitudes, because some conductivity anomalies are shallower than the depth of anisotropy. Sometimes these distortions are corrected using geomagnetic transfer functions derived from the daily fluctuations of the magnetic field generated by current vortices in the ionosphere (*4, 10, 11*). However, electromagnetic source field heterogeneities (*12*) hinder the estimation of geomagnetic transfer functions at periods above 10,000 s in Scandinavia, rendering this correction technique inapplicable. Instead, we made use of the conductivity increase at the olivine-wadsleyite transition at 410 km depth, which is evident in laboratory conductivity data (*13*) and in mantle conductivity models obtained from the geomagnetic daily variations (*3*), to estimate the depth to the direction-dependent conductive structure at two sites. The result, z = 180 km, agrees with seismic determinations of the thickness of the Fennoscandian lithosphere (*14*). At other sites, because of the large conductance, the electromagnetic field in the high-conductivity direction does not penetrate down to 410 km even at the longest period, 10,000 s. However, the coincidence with the seismic results at two sites, and with the depth of the anisotropic conductor at neighboring electromagnetic sites, suggests that the direction-dependent conductivity structure is located at the base of the lithosphere. The anisotropic structure under Australia was found to be deeper than 150 km (*4*).

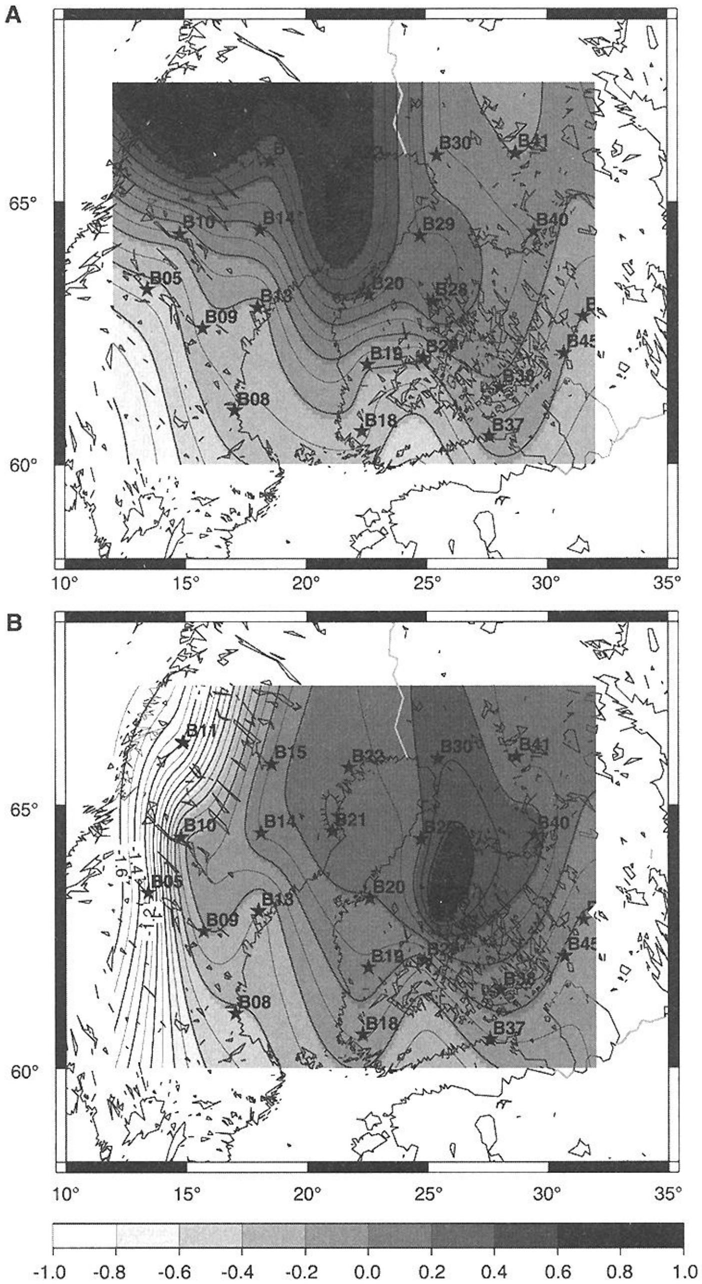

Fig. 2. Isolines of the geomagnetic transfer functions $(B_x - B_{xn})/B_{xn}$ and $(B_y - B_{yn})/B_{yn}$ (relative spatial variations of the amplitudes of the x and y component of geomagnetic variational fields, respectively) at all sites for the period 2049 s. The magnetic reference field B_n was measured at site B22.

The electromagnetic strike can be influenced by macroscopic structures (*15*) in the lithosphere, and mantle anisotropy in the uppermost 100 km of the mantle has been interpreted in terms of graphite preserved in shear zones (*2*). However, electrical anisotropy at the base of the lithosphere (as detected below Australia and Fennoscandia) may arise as a result of grain-scale enhancement of the conductivities, because macroscopic structural lineaments are unlikely to be preserved under the deformation conditions expected at the base of the lithosphere (*16*). On the other hand, the temperature dependence of hydrogen diffusivity (*5*) could explain why this conduction mechanism is more dominant at the base of the lithosphere than at shallower depths.

If the depth of a conductive structure is known, its conductance can be calculated from the phase in a particular period band (*10, 17*) (Table 1). The conductances in the maximal-conductivity direction and in the minimal-conductivity direction (τ_{max} and τ_{min}) determined for the Australian upper mantle lie between those determined for the upper mantle below Fennoscandia. The maximum conductances of two European sites (*3*)

Table 1. Period T at which the approximate conductance estimation is centered, conductance τ_{max} in the maximal-conductivity direction, and conductance τ_{min} in the minimal-conductivity direction for sites in Central Australia (*4*), Fennoscandia, and Northern Bavaria (Central Europe) (*3*). The symbol ">" indicates that only a lower bound of the conductance can be computed because of the limited period range (*10, 17*); "<200" indicates that no conductance can be resolved, although the data should resolve any conductance larger than 200 S.

Site	T (s)	τ_{max} (S)	τ_{min} (S)
Australia			
WRA	3,000	8,100	3,000
DOR	3,000	7,500	3,000
Fennoscandia			
B39	3,000	>7,000	<200
B19	4,000	>32,000	<200
Northern Bavaria (Central Europe)			
KHF	500	1,700	<200
GAM	500	1,900	<200

are much smaller, but a preliminary analysis of a larger data set suggests that this result is not representative (*18*). There is a discrepancy between the anisotropy factors (i.e., the τ_{max}/τ_{min} ratios): The fast-moving (*19, 20*) Australian plate has a small anisotropy factor of 2.7, whereas the slow-moving North European plate exhibits maximum anisotropy factors of 35 to 100 under Fennoscandia. This result is surprising, because geodynamic models suggest that the greater the strain imparted on the mantle by an overriding tectonic plate, the greater the expected degree of alignment of olivine crystals in the direction of plate motion. Therefore, a greater degree of alignment should be expected below the Australian plate than below the Fennoscandian plate if electrical anisotropy is linked to present-day plate motion. In both target areas, the high-conductance directions coincide with seismic fast directions (*7, 9*). We suggest that the anisotropy detected in the mantle below the Fennoscandian plate is either a relic of paleoflow in the mantle, induced at a time when the mantle in this region was subjected to a larger strain, or is indicative of sublithospheric convection dominating mantle flow (*16*). If the alignment is preserved over geological time scales, this would imply that the relaxation time of the mantle is more than 10^7 years and longer than hitherto believed, providing a useful constraint on geodynamic models for convective flow (*21*) and the evolution of lattice-preferred orientation in olivine aggregates.

References and Notes

1. J.-P. Montagner, T. Tanimoto, *J. Geophys. Res.* **96**, 20337 (1991).
2. M. Mareschal *et al.*, *Nature* **375**, 134 (1995).
3. K. Bahr, A. Duba, *Earth Planet. Sci. Lett.* **178**, 87 (2000).
4. F. Simpson, *Nature* **412**, 632 (2001).
5. S. J. Mackwell, D. L. Kohlstedt, *J. Geophys. Res.* **95**, 5079 (1990).
6. S.-I. Karato, *Nature* **347**, 272 (1990).
7. E. Debayle, B. L. N. Kennett, *J. Geophys. Res.* **105**, 25423 (2000).
8. The confidence intervals of the electromagnetic strike angle are estimated by applying the error propagation law to the formula that links the strike angle to the elements of the magnetotelluric impedance tensor (*4*).
9. L. P. Vinnik, L. I. Makeyeva, A. Milev, A. Yu. Usenko, *Geophys. J. Int.* **111**, 433 (1992).
10. K. Bahr, M. Bantin, Chr. Jantos, E. Schneider, W. Storz, *Phys. Earth Planet. Inter.* **119**, 237 (2000).
11. U. Schmucker, *Phys. Earth Planet. Inter.* **7**, 365 (1973).
12. I. L. Osipova, S. E. Hjelt, L. L. Vanyan, *Phys. Earth Planet. Inter.* **53**, 337 (1989).
13. Y. Xu, T.-J. Shankland, B. T. Poe, *J. Geophys. Res.* **105**, 27865 (2000).
14. P. Suhadolc, G. F. Panza, St. Mueller, *Tectonophysics* **176**, 123 (1990).
15. F. Simpson, *J. Geophys. Res.* **105**, 19321 (2000).
16. H. Schmeling, G. Marquart, *Phys. Earth Planet. Inter.* **79**, 241 (1993).
17. For a three-layer model consisting of a resistive lithosphere of thickness h, a conductive sublithospheric layer of conductance τ, and a moderately resistive (100 ohm · m) upper mantle in which the electromagnetic field at an angular frequency ω has a penetration depth p, both the real (Re) and imaginary (Im) parts of the Schmucker-Weidelt transfer function $C(\omega)$ at this frequency are polynomials in $\omega\mu_0\tau p$ (*10*), where μ_0 is free space permeability. For conductances τ that are so large that $\omega\mu_0\tau p \gg 1$, the magnetotelluric phase ϕ is linked to the model parameters by

$$\tan(\phi) = -\frac{\mathrm{Re}\,C}{\mathrm{Im}\,C} = \omega\mu_0\tau h$$

Here, h is estimated after solving the static shift problem of magnetotellurics (e.g., by extension to long periods) or by a comparison to a reference model. If h is known, then τ can be computed from ϕ for periods short enough to ensure that $\omega\mu_0\tau h \gg 1$ but long enough to ensure that Re $C > h$ (*10*). If the second condition is violated, then the resulting conductance is a lower bound of the actual conductance.
18. A. Gatzemeier, personal communication.
19. A. E. Gripp, R. G. Gordon, *Geophys. Res. Lett.* **17**, 1109 (1990).
20. S. Wang, R. Wang, *Earth Planet. Sci. Lett.* **189**, 133 (2001).
21. É. Kaminski, N. M. Ribe, *Earth Planet. Sci. Lett.* **189**, 253 (2001).

22. Data acquisition with the German long-period magnetotelluric cluster in Scandinavia was made possible by the German Science Foundation under contract Ba 889/8 and an internal grant from Geoforschungszentrum Potsdam. We thank F. Echternacht, M. Engels, E. Eggert-Heise, T. Korja, J. Leibecker, K. Roden, and E. Steveling for organizing the field campaign.

10 September 2001; accepted 7 January 2002

A Microphysical Connection Among Biomass Burning, Cumulus Clouds, and Stratospheric Moisture

Steven Sherwood

A likely causal chain is established here that connects humidity in the stratosphere, relative humidity near the tropical tropopause, ice crystal size in towering cumulus clouds, and aerosols associated with tropical biomass burning. The connections are revealed in satellite-observed fluctuations of each quantity on monthly to yearly time scales. More aerosols lead to smaller ice crystals and more water vapor entering the stratosphere. The connections are consistent with physical reasoning, probably hold on longer time scales, and may help to explain why stratospheric water vapor appears to have been increasing for the past five decades.

Data collected during the last half-century appear to indicate an approximate doubling of stratospheric water vapor during this period, of which approximately half can be accounted for by increases in stratospheric production of water vapor by methane oxidation (*1*). The other half presumably results from increases in the moisture content of air entering the stratosphere through the tropical tropopause. However, temperatures near this entry point, which were thought to regulate stratospheric moisture levels, have not increased during recent decades (*2, 3*). This implies that either relative humidity near the tropopause has substantially increased, or other pathways exist whereby moisture can enter the stratosphere. The importance of this problem is underscored by recent findings that stratospheric moisture increases may be a significant contributor to global temperature trends (*4*) and may also interfere with the recovery of polar ozone by exacerbating destruction mechanisms (*5*).

I show that fluctuations in stratospheric humidity can indeed be caused by fluctuations in relative humidity just below the tropical tropopause, which in turn are governed by the sizes of ice crystals lofted in deep convective updrafts. The moisture content of air entering the stratosphere is thought to be controlled by condensation of vapor to the ice phase in transient lifting events outside of convective cells and/or phase changes within intense convective cells themselves (*6*). The relative importance of these two controlling factors is unknown. Convective moistening or drying should depend not only on temperature but also on the propensity of lofted ice to evaporate at a level high enough (>14 to 15 km) so that the vapor will enter the stratosphere rather than subsiding back into the troposphere (*7, 8*). It has been widely assumed that condensation outside of convection resets the water vapor to a lower value independent of convective influence, but the evidence presented here argues against this assumption.

This study uses data acquired from 1992 to 1998. Ice crystal "effective diameter" D_e was retrieved near the tops of deep cumulonimbus clouds (Cb) using the ISCCP (International Satellite Cloud Climatology Project) B3 archive of radiance observations by the AVHRR (Advanced Very High Resolution Radiometer) on

Department of Geology and Geophysics, Yale University, New Haven, CT 06520, USA. E-mail: steven.sherwood@yale.edu